

Attenuation length of low energy electrons in Oxide thin films

S. Iacobucci¹, F. Offi², P. Torelli³, L. Petaccia⁴

¹ *CNR - Istituto di Struttura della Materia (ISM) c/o Dipartimento di Scienze Università degli Studi Roma Tre, Via della Vasca Navale 84, I-00146 Roma (Italy)*

² *Dipartimento di Scienze, Università degli Studi Roma Tre, Via della Vasca Navale 84, I-00146 Roma, Italy*

³ *CNR- Istituto Officina dei Materiali, TASC Laboratory, Strada Statale 14 km 163.5, I-34149 Trieste, Italy*

⁴ *Elettra Sincrotrone Trieste, Strada Statale 14 km 163.5, I-34149 Trieste, Italy*

(24th September 2018)

Abstract

The effective attenuation length (EAL) of electrons in MgO films has been measured in the (5.5-28) eV energy range by the over-layer method and correlated with the band structure of the material. As expected the EAL is found to increase when lowering the electron energy, but the obtained values are smaller than predictions based on the universal curve. The comparison of the experimental results with optical properties calculations available in literature suggests that, for energies lower than 20 eV, the relevant scattering mechanisms are described by the imaginary part of the dielectric function, accounting in particular for the steep increase of the EAL for energies lower than the insulator band gap.

Introduction

Ever since the early development of electron spectroscopies (ES), there was interest in the quantitative estimation of the depth probed in the experiments and it was soon evident that in the most commonly used energy range of ES (from few tens of eV to about 1.5 keV) the information is confined within the outermost few layers.¹ This surface sensitivity poses a limitation for the investigation of systems where the electronic structure differs from the bulk one, such as strongly correlated materials, buried interfaces and capped samples. Overcoming this limitation has pushed to apply ES, and photoemission spectroscopy (PES) in particular, out of its conventional energy range, relying on the expected decrease of the electron scattering probability at very low (less than about 10 eV) and very high (more than several keV) electron kinetic energy E . This issue is summarized in the “universal curve” (UC) that predicts an increase of the electron inelastic mean free path (IMFP) in these two energy regimes.² In particular, application of PES in the low energy range has experienced a revival, since this approach enables an outstanding energy resolution,³ thus

allowing experiments on systems featuring structures of the energy spectral function as narrow as few meV, such as strongly correlated electron systems and, among them, superconductors.⁴

However, bulk sensitivity at very low energy is especially questionable for materials that are not classified in the category of “elements” in the original publication of Seah and Dench.² Thus it appears as an oversimplification the use of the UC for, e.g., inorganic compounds, even as a rule of thumb, since only a little number of experimental points was available for the fit with the $1/E^2$ energy dependence. Furthermore, and more precisely, the predictive formula has indeed to be considered as an empirical curve only and the quantification of the surface/bulk sensitivity of PES needs to account for several factors such as material dependence, electron scattering mechanism, experimental geometry, etc.⁵

Indeed, the determination of the bulk sensitivity of low-energy PES is still an open issue, because the scattering properties of electrons in this energy range are not well known.⁶ Recent experiments performed both on rare earth films⁷ and insulators,^{8,9} as well as in organic semiconductor films,¹⁰ have shown the effective attenuation length (EAL) of slow electrons does not increase so much as expected according to the predictive formula.² The material dependence of the IMFP at low energies was already pointed out in the case of ferromagnetic thin films¹¹ together with spin asymmetry of the electron transport highlighted for very slow electrons (about 1eV) in the case of tunneling magnetic interfaces.^{12,13} In addition, limitation in the bulk sensitivity of low-energy PES with respect to high-energy PES is reported for selected examples of strongly correlated materials.¹⁴

From the theoretical point of view, the material dependence of the EAL, which is identifiable with the IMFP if elastic scattering effects are negligible, was already shown.¹⁵ Calculations indicated that differences between EAL and IMFP is dependent on electron energy;¹⁶ and this difference increases with decreasing electron energy.¹⁷ In particular, the effect of the material electronic structure was highlighted in calculation of IMFP of several elements for $E > 50\text{eV}$ and correlated with the plasmon excitations. However the free-electron gas approximation used at high energy for predicting electron IMFPs¹⁸ is no longer valid at low energies, as the band structure effects become significant: for electron energies lower than 20 eV the probability of plasmon excitations vanishes, valence – conduction band transitions (together with phonon excitations) become the major channel for inelastic scattering of electrons, hence the rate of the energy loss is determined by the imaginary part of the dielectric function.¹⁹ This has been pointed out in recent IMFP studies of a number of materials over a wide energy range, based on the results of first-principles calculations or experimental data available at low energies.²⁰ In particular it is of relevant interest to discern the possible effect of the energy gap E_g in determining the IMFP in the low

energy range. Such effects are accounted for in refined theoretical models and in specific calculations including spin-transport properties of transition metals,²¹ and compared with PES experiment on Be and Al²².

In this scenario, an interesting material candidate to be investigated is MgO, a large gap ($E_g^{MgO} = 7.77$ eV) insulator,²³ which belongs to a specific class of systems that have attracted much attention like metal oxides-semiconductor heterostructures, whose tunnel contacts are of considerable technological importance. It has been shown that to determine via PES the energy band structure of the buried MgO/semiconductor interface is of crucial importance for a complete understanding of the fundamental transport mechanism of spin polarized electrons through the tunnel contact.²⁴ Furthermore, Altieri et al. have pointed out how the insulating character of a MgO capping layer could play a fundamental role in the process enhancing the slow electrons yield in X-ray absorption experiments on NiO films.²⁵

Among the experimental methods addressing direct measurement of the EAL in MgO it is worth mentioning the work of Fecher et al., who used valence band spectra to estimate the EAL of the electrons through the insulator layer to be 17 nm at kinetic energies of about 6 keV.²⁶ Yet, there is a lack of experimental data available in the low energy regime and an experimental determination of the EAL of slow electrons in MgO films would allow for a direct comparison with the corresponding results⁸ on a small-gap insulator like CoO ($E_g^{CoO} = 2.5$ eV).²⁷

Experimental methods

A wedge-shaped MgO/Ag sample prepared ex-situ in the MBE preparation chamber of the APE beamline has been characterized and measured at the BaDElPh beamline of the Elettra synchrotron (Trieste, Italy).²⁸ Namely, the substrate was a silver single crystal with the (001) surface plane with rectangular shape and borders parallel to the $\langle 110 \rangle$ direction of the fcc Ag lattice. The substrate was prepared by repeated cycles of sputtering (Ar⁺ ions of 600 eV of kinetic energy) and annealing (at 670 K for 20 minutes). The quality of the surface after the preparation procedure was verified by low-energy electron diffraction (LEED). On the clean surface we evaporated MgO by molecular beam epitaxy from MgO target. The rate employed was 0.58 angstrom per minute obtained with a quartz crystal oscillator. To obtain the maximum precision in the determination of the thickness the rate was verified by photoemission experiments on a reference sample (i.e. we evaporated a MgO film of 1 nm of thickness on GaAs, system in which we had calibrated the deposit thickness by XPS and by TEM in a previous experiment²⁹). Successively, films of variable thickness (7, 10, 20, 50, 100 angstrom) were deposited in a stair like

structure as sketched in Fig. 1 (left panel), each step being about 1mm wide. Films obtained by such a procedure are epitaxial with Ag[100]//MgO[100] and show MgO(001) surfaces with large flat terraces.³⁰

The wedge-shaped sample was transferred to the BaDElPh experimental station, where the MgO surface was restored by in-situ annealing for one hour at 470 K, obtaining the same conditions of the sample immediately after preparation, for what concerns cleanliness and crystallographic order, as verified by X-ray photoemission spectroscopy (XPS) and LEED. Vanishing of the C 1s signal and O 1s peak narrowing after annealing with respect to the as-introduced sample were indicators of the surface cleanliness. LEED measurements at 60 eV kinetic energy revealed (1x1) patterns for all the MgO coverages, sharp up to 50 angstrom thickness and visible up to 100 angstrom (Fig. 1, right panel), thus testifying the epitaxial growth and the long range order of the sample surface.

Normal emission PES spectra were taken at room temperature as a function of the photon energy in the range (5.5-28) eV, measuring the intensity of the Fermi level of the Ag substrate for each MgO thickness with a fixed angular acceptance of the analyzer of $\pm 7^\circ$. Reference signal from the clean Ag surface was obtained after sputtering and annealing the sample in-situ and by measuring PES spectra as a function of the photon energy. In order to benchmark measurements on the MgO sample grown ex-situ, a 30 angstrom thick MgO film was grown in-situ on the clean Ag substrate. The resulting PES spectra were in line with the ones of the sample grown ex-situ. By repeating the XPS characterization and the PES measurements after one day we checked film stability and experiment reproducibility.

Results and Discussion

PES spectra in the Fermi level region have been measured in the $h\nu = (5.5-28)$ eV photon energy range as a function of the MgO coverage. In Fig. 2 the electron distribution curves (EDC's) measured for photon energies $h\nu=7$ eV (upper panel) and $h\nu=28$ eV (bottom panel) are displayed, respectively. In the figure only the last 0.5 eV close to the Fermi level are displayed; in this energy interval (well inside the MgO band gap) only the Ag state contribute to the photoemission intensity thus making possible to easily appreciate the attenuation from the MgO overlayer. Two qualitative evidences are worth considering: i) a fast attenuation of the Fermi level signal from the Ag substrate for increasing MgO thickness is evident for both photon energies; ii) the attenuation is less pronounced in the low photon energy spectrum. It is noticeable that 7eV is lower than the insulator optical gap $E_g^{MgO}=7.77$ eV.²³

To estimate the EAL, a quantitative analysis has been performed on the spectra measured at each photon energy. An example of the procedure used to derive the EAL is reported in Fig. 3 for a spectrum at $h\nu = 9\text{eV}$. The de-convolution of the PES spectrum for the film of 7\AA thickness is shown in the upper panel: the intensity at the Fermi level is extracted as the integral intensity of the Fermi function obtained from the EDC after subtracting a flat background and the residual intensity of the Ag(100) surface resonance.³¹ The integral is calculated between the two energy values corresponding to 10% and 90% of the Fermi function edge. The Fermi level intensities, obtained by applying the same de-convolution for each MgO coverage, are reported in the bottom panel of Fig. 3, where an exponential decay function is used to fit data and to derive the EAL for $h\nu = 9\text{eV}$.

By repeating such procedure for all spectra measured at different photon energies, a dependence of the EAL vs electron energy is achieved and it is displayed in Fig. 4 with error bars obtained from the fitting procedure. The electron energy is referred to the Fermi level (zero of the energy scale), hence it coincides with the photon energy. A comparison with the corresponding results for CoO⁸ is also shown. In the measured range, the EAL for MgO is characterized by an increase at low energy (less than 10eV) and by a broad bump at higher energies centered at about 17 eV. The EAL of MgO steeply increases for photon energies below about 8 eV that is a value close to the material band gap. Note however that such augment is lower than the average behavior suggested by the UC for inorganic compounds (also displayed in Fig. 4), which would predict a value of about 25 Å for $E = 8\text{ eV}$.² This slow slope of the EAL at low energy, less steep than expected, was also observed for CoO,⁸ thus, as a general observation, the curve tabulated by Seah and Dench overestimates what experimentally observed; furthermore, a pronounced material dependence is evident in the experimental data. Indeed, as shown in Fig. 4, the EAL of CoO are quite lower than the one of MgO and the increase starts at lower energies: this result can be correlated with the different energy gaps of the two materials. To put this observations on a more quantitative ground, we fit the experimental data for $E < 15\text{eV}$ with the curve $EAL(E) \approx$

$\frac{\sqrt{E}}{a(E - E_{th})^b}$ proposed by Ziaja et al.,³² where E_{th} is the effective threshold for pair production (which may possibly differ from the energy gap E_g), and where a and b are coefficients that depend strongly on the details of the band structure of the solid. The results of the fitting procedure are shown as continuous lines in Fig. 4: the fitting values of the two coefficients a and b are quite different for MgO ($a_{\text{MgO}} = (7 \pm 4) 10^{-5}$; $b_{\text{MgO}} = 3.8 \pm 0.3$) and for CoO ($a_{\text{CoO}} = (4 \pm 7) 10^{-3}$; $b_{\text{CoO}} = 1.9 \pm 0.9$). Within the large uncertainties for the CoO coefficients, due to the larger error bars of the experimental data, we observe that the marked difference for the b-values of CoO and MgO are in line with the different insulating character of the two materials. Namely, according to the free-

electron-gas model of solids one should expect $b = 2$ in the case of metals; as a crude approximation, deviations from this value are expected to reflect dissimilarities of the Fermi surface of the material with respect to a sphere; in particular, referring to metals as “zero-gap materials”, a larger deviation is expected for MgO with respect to CoO, on the basis of its larger energy gap.

The discussion of the EAL energy dependence for MgO deserves further analysis. In Fig. 5 the results of our experiment are compared with the dielectric function calculated by Kohiki et al.³³ The reciprocal of the MgO EAL is plotted on the same energy scale of both the imaginary part of the dielectric function (and directly compared with it in the upper panel of Fig. 5) and the loss function (bottom panel). The comparison is meaningful, insofar the photoelectron IMFP is usually derived by using a relation firstly suggested by Ritchie,³⁴ linking it to the electron self-energy and, hence, to the dielectric response function.¹⁹ The agreement between our data and the calculated absorption part of the optical constants is good up to 17eV, thus experimentally benchmarking the Quinn’s model cited in the introduction;¹⁹ and it is excellent in the very-low energy range (less than 10eV), where the experimental points are well reproduced by the calculated optical profile, thus reflecting the band structure effects and the energy gap appearance in particular.²⁰ For higher energy a large discrepancy is evident between our data and the imaginary part of the dielectric function: for energies greater than 20 eV a significant contribution due to collective excitations as possible scattering channels for the photo-emitted electrons is expected, and a comparison of our experimental results could be attempted with the loss function by correlating the increase of the reciprocal of the EAL with the plasmon feature reported at about 23 eV.^{33,35}

Conclusions

We have measured the effective attenuation length of slow electrons in MgO and compared it with results of a similar experiment on CoO.⁸ We have found that the effective attenuation length of MgO increases at low energies and, although higher than CoO, it is anyway lower than expected according to the universal curve.² By correlating our results with the band structure, specifically we have found a steep increase for energies lower than the insulator optical gap of MgO. In a regime where inelastic mean free paths are difficult to determine experimentally,³⁶ a favorable comparison of our results with a band structure calculation, like the one used in³³ to model the optical properties of MgO, highlights how the absorption part of the dielectric function can be directly correlated with the measured effective attenuation length at very low energy.

Acknowledgments

Two of us (S.I. and F.O.) gratefully acknowledge the Support for Italian Users of Elettra synchrotron facility.

Fig.1. (Left) Sketch of the stair-like structure of the wedged-thickness MgO sample grown ex-situ on Ag (100) single crystal. (Right) LEED pattern measured at 60 eV of kinetic energy for the thinnest (upper panel) and for the thickest (bottom panel) MgO coverage.

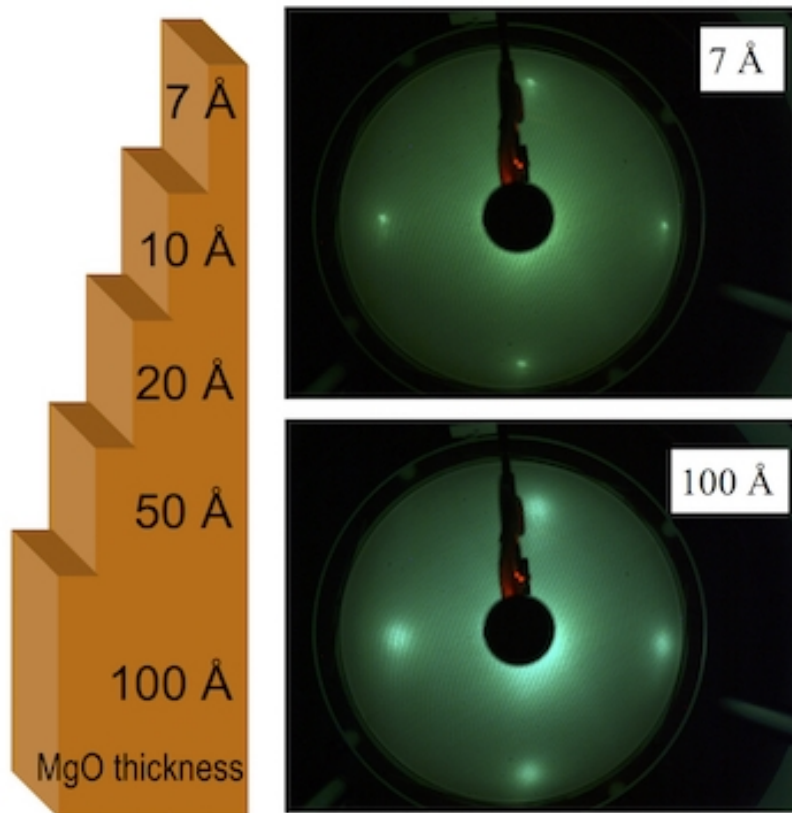


Fig. 1

Fig. 2. PES spectra measured in the Fermi level E_F region of Ag for two selected photon energies $h\nu=7\text{eV}$ and $h\nu=28\text{eV}$ as a function of the indicated MgO coverage.

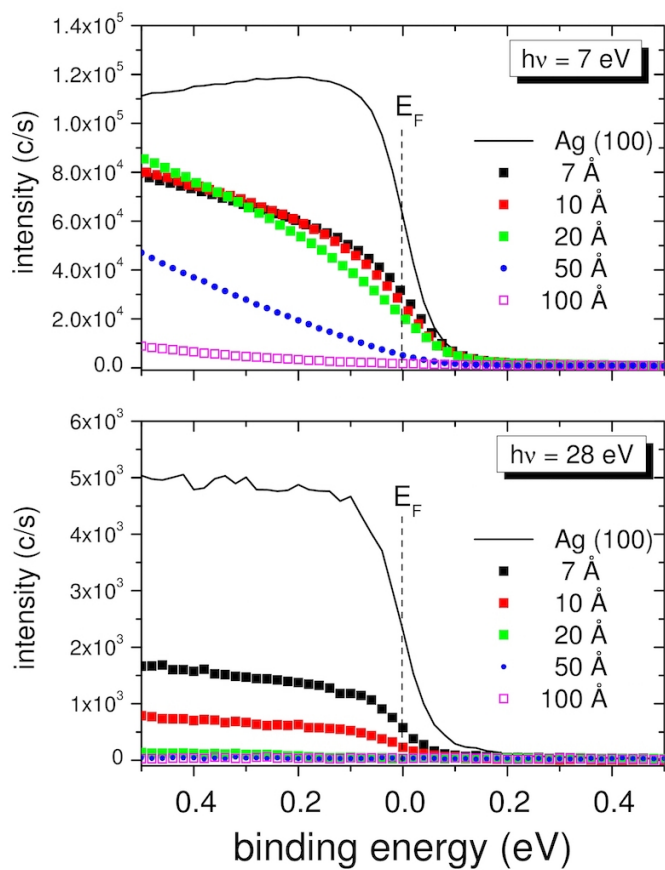


Fig. 2

Fig. 3. Upper panel: an example of the procedure used to extract the signal at the Fermi level for $h\nu=9\text{eV}$. PES spectrum measured on the 7\AA MgO coverage (black squares) and its best fit (grey line); the gross Fermi edge profile (blue line) obtained after removing the residual component of the Ag(100) surface resonance³¹ (cyan lines) and the net Fermi edge profile (red line) after subtracting the linear background. Bottom panel: integrated intensity (between 10% and 90% of the Ag Fermi edge profile reported as a function of the MgO coverage (red circles); the exponential decay fitting function used to derive the EAL is also shown (red line).

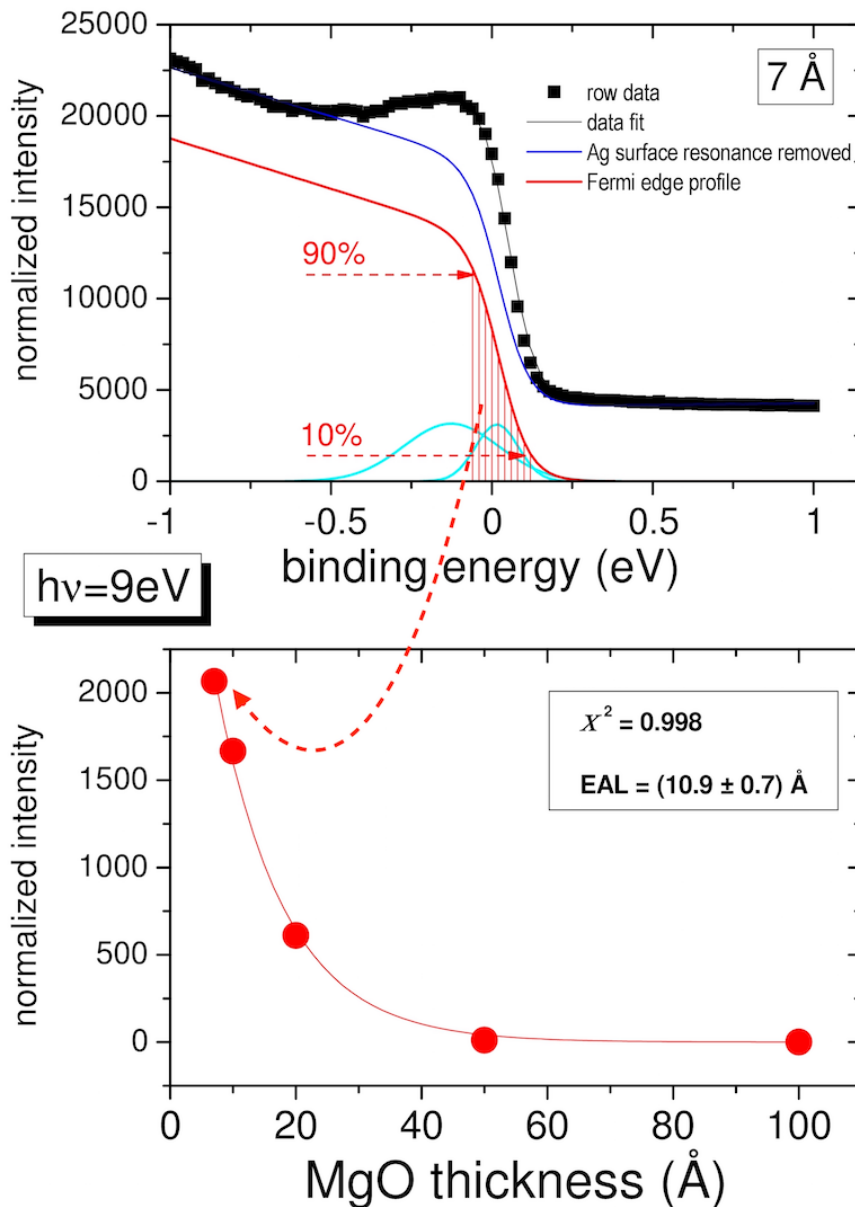


Fig. 3

Fig. 4. Experimental effective attenuation length for MgO: results of the present work (pink circles) are compared with the corresponding results of the experiment on CoO⁸ (empty green circles). The continuous lines are the best fits of data in the low energy range (see text for details). The Seah-Dench “universal curve” for inorganic compounds² is also shown (black dashed line).

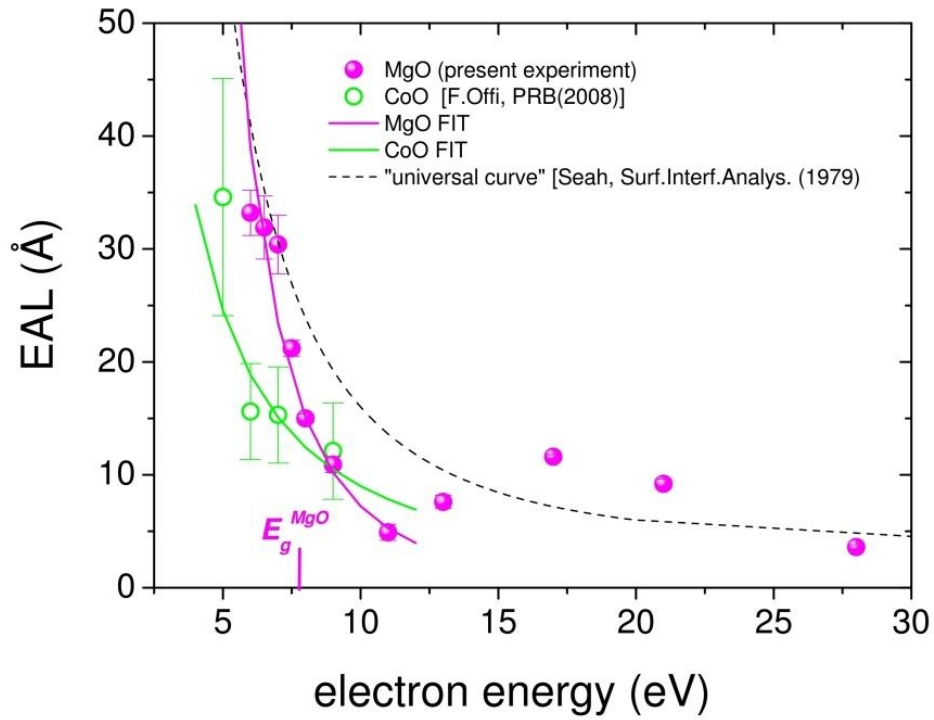


Fig. 4

Fig. 5. Comparison of the EAL data with optical properties calculation³³. Upper panel: the reciprocal of the EAL data derived in the present experiment for MgO (pink circles) and the calculated imaginary part of the dielectric function (green line). Bottom panel: surface (red line) and bulk (black line) loss function are plotted on the same energy scale.

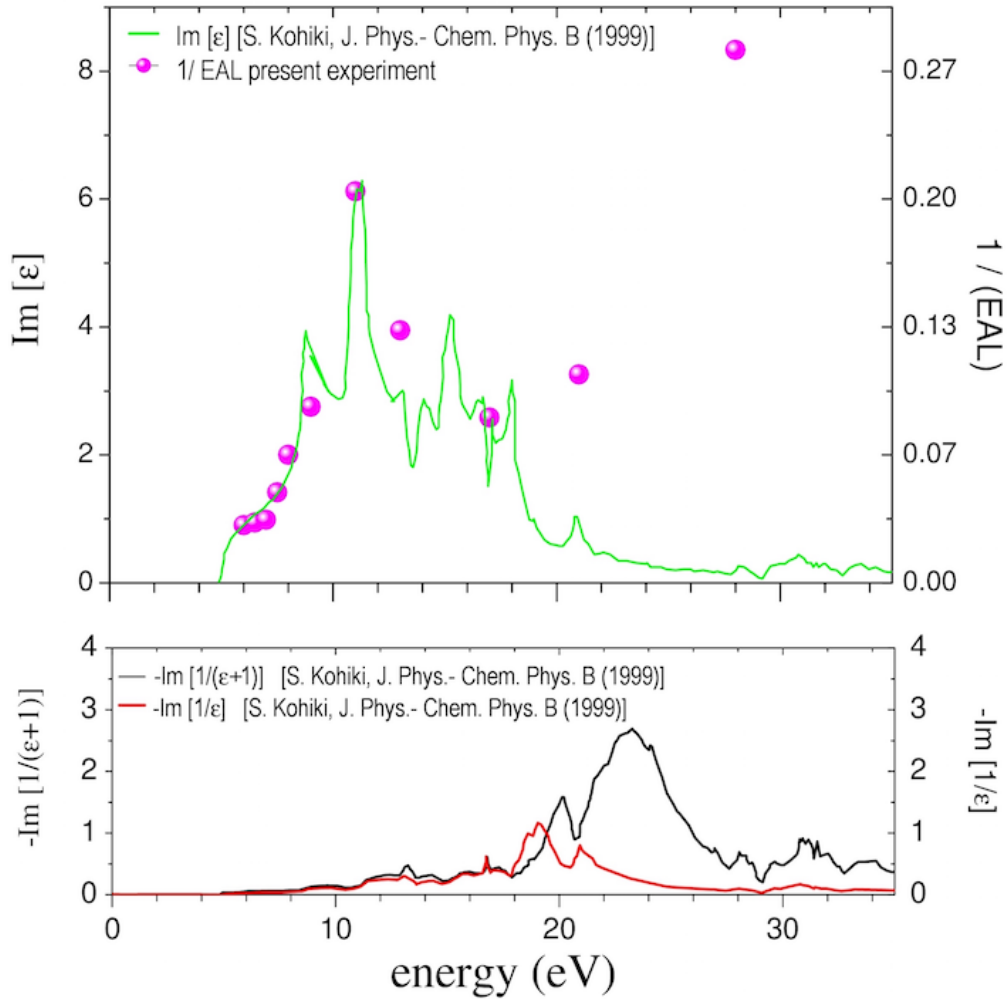


Fig. 5

References

- ¹ Y. Baer, P. F. Heden, J. Hedman, M. Klasson, C. Nordling, *Solid State Commun.* 8 (1970) 1479.
- ² M. P. Seah and W. A. Dench, *Surf. Interface Anal.* 1 (1979) 2.
- ³ T. Kiss, F. Kanetaka, T. Yokoya, T. Shimojima, K. Kanai, S. Shin, Y. Onuki, T. Togashi, C. Zhang, C. T. Chen, and S. Watanabe, *Phys. Rev. Lett.* 94 (2005) 057001.
- ⁴ N. C. Plumb et al. *Phys. Rev. Lett.* 105, 046402 (2010); M. Mulazzi et al., *Phys. Rev. B* 82 (2010) 075130.
- ⁵ C. J. Powell and a: Jablonski, *Nucl. Instrum. Meth. A* 601 (2009) 54.
- ⁶ S. Tougaard, J. Kraaer, *Phys. Rev. B* 43 (1991) 1651.
- ⁷ F. Offi, S. Iacobucci, L. Petaccia, S. Gorovikov, P. Vilmercati, A. Rizzo, A. Ruocco, A. Goldoni, G. Stefani and G Panaccione, *J. Phys.: Condens. Matter*, 22 (2010) 305002.
- ⁸ F. Offi, S. Iacobucci, P. Vilmercati, A. Rizzo, A. Goldoni, M. Sacchi, and G. Panaccione, *Phys. Rev. B* 77 (2008) 201101 (R).
- ⁹ F. C. Marques, J. J. Jasieniak, *Appl. Surf Sci.* 422 (2017) 504–508.
- ¹⁰ Y. Ozawa, Y. Nakayama, S. Machida, H. Kinjo, H. Ishii, *J. Electron. Spectrosc. Relat. Phenom.* 197 (2014) 17–21.
- ¹¹ D. P. Pappas, K.-P. Kämper, B. P. Miller, H. Hopster, D. E. Fowler, C. R. Brundle, A. C. Luntz, and Z.-X. Shen, *Phys. Rev. Lett.* 66 (1991) 504.
- ¹² S. van Dijken, X. Jiang and S. S. P. Parkin, *Phys. Rev. B* 66 (2002) 094417.
- ¹³ R. Fetzer B. Stadtmüller, Y. Ohdaira, H. Naganuma, M. Oogane, Y. Ando, T. Taira, T. Uemura, M. Yamamoto, M. Aeschlimann,, M. Cinchetti, *Sci. Rep.* 5 (2015) 8537; DOI: 10.1038/srep08537.
- ¹⁴ S. Suga, T. Tusche, *Journal of Electron Spectrosc. Relat. Phenom.* 200 (2015) 119–142
- ¹⁵ A. Jablonski, C.J. Powell, *Surf. Sci. Rep.* 47 (2002) 33; A. Jablonski, C. J. Powell, *Journal of Electron Spectrosc. Relat. Phenom.* 100 (1999) 137.
- ¹⁶ Y F Chen, C M Kwei and C J Tung, *J. Phys. D: Appl. Phys.* 25 (1992) 262.
- ¹⁷ A. Jablonski, *Surf. Sci.* 188 (1987) 164.
- ¹⁸ S. Tanuma, C. J. Powell, D. R. Penn, *Surf. Interf. Analysis* 17 (1991) 911.
- ¹⁹ J. J. Quinn, *Phys. Rev.* 126 (1962) 126.
- ²⁰ B. Ziaja, Richard A. London, Janos Hajdu, *J. Appl. Phys.* 99 (2006) 033514.
- ²¹ V. P. Zhukov, E. V. Chulkov, and P. M. Echenique, *Phys. Rev. B* 73 (2006) 125105.
- ²² E. E. Krasovskii, V. M. Silkin, V. U. Nazarov, P. M. Echenique, and E. V. Chulkov, *Phys. Rev. B* 82 (2010) 125102.

-
- ²³ D. M. Roessler and W. C. Walker, *Phys. Rev.* 159 (1967) 733.
- ²⁴ K.-R. Jeon, S.-J. Lee, C.-Y. Park, H.-S. Lee, and S.-C. Shin, *Appl. Phys. Lett.* 97 (2010) 111910.
- ²⁵ S. Altieri, M. Finazzi, H.H. Hsieh, H.-J. Lin, C.T. Chen, S. Valeri, L.H. Tjeng, *Surf. Sci* 604 (2010) 181.
- ²⁶ H. Fecher, B. Balke, A. Gloskowskii, S. Ouardi, C. Felser, T. Ishikawa, M. Yamamoto, Y. Yamashita, H. Yoshikawa, S. Ueda, and K. Kobayashi, *Appl. Phys. Lett.* 95 (2008) 193513.
- ²⁷ J. van Elp, J. L. Wieland, H. Eskes, P. Kuiper, G. A. Sawatzky, F. M. F. de Groot, and T. S. Turner, *Phys. Rev. B* 44 (1991) 6090.
- ²⁸ L. Petaccia, P. Vilmercati, S. Gorovikov, M. Barnaba, A. Bianco, D. Cocco, C. Masciovecchio, and A. Goldoni, *Nucl. Instrum. Meth.A* 606 (2009) 780.
- ²⁹ P. Torelli, M. Sperl, R. Ciancio, J. Fujii, C. Rinaldi, M. Cantoni, R. Bertacco, M. Utz, D. Bougeard, M. Soda, E. Carlino, G. Rossi, C. H. Back and G. Panaccione, *Nanotechnology* 23 (2012) 465202.
- ³⁰ P. Torelli, S. Benedetti, P. Luches, L. Gagnaniello, J. Fujii, and S. Valeri, *Phys. Rev. B* 79 (2009) 035408.
- ³¹ E. D. Hansen, T. Miller, and T.-C. Chiang, *Phys.Rev. B* 55 (1997) 1871.
- ³² B. Ziaja, R. A. London, and J. Hajdu, *J. Appl. Phys.* 99 (2006) 033514.
- ³³ S. Kohiki, M. Arai, H. Yoshikawa, S. Fukushima, *J. Phys. Chem. B* 103 (1999) 5296.
- ³⁴ R. H. Ritchie, *Phys. Rev.* 114 (1959) 644.
- ³⁵ A. Schleife, C. Rödl, F. Fuchs, J. Furthmüller, and F. Bechstedt, *Phys. Rev. B* 80 (2009) 035112.
- ³⁶ C. J. Powell, *J. Electron Spectrosc.* 47 (1988) 197.

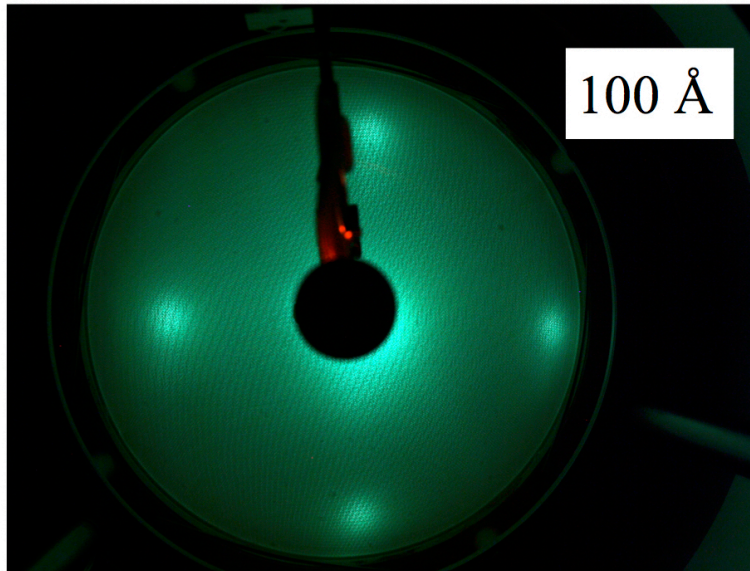
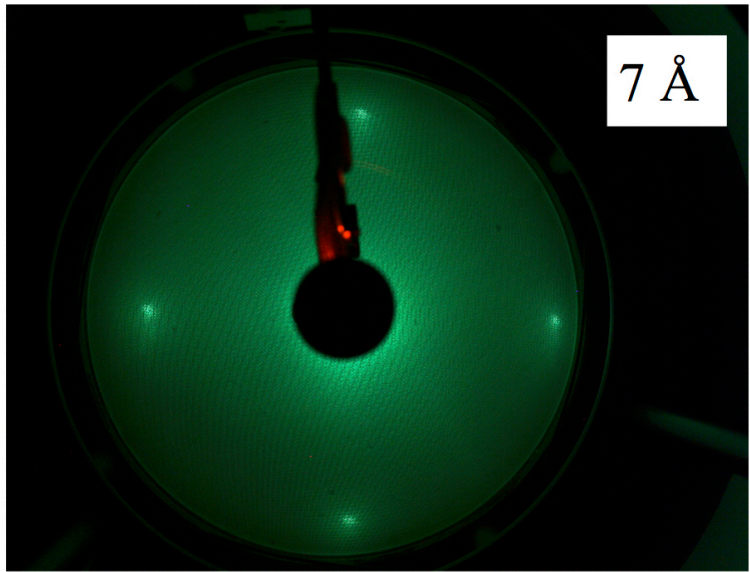
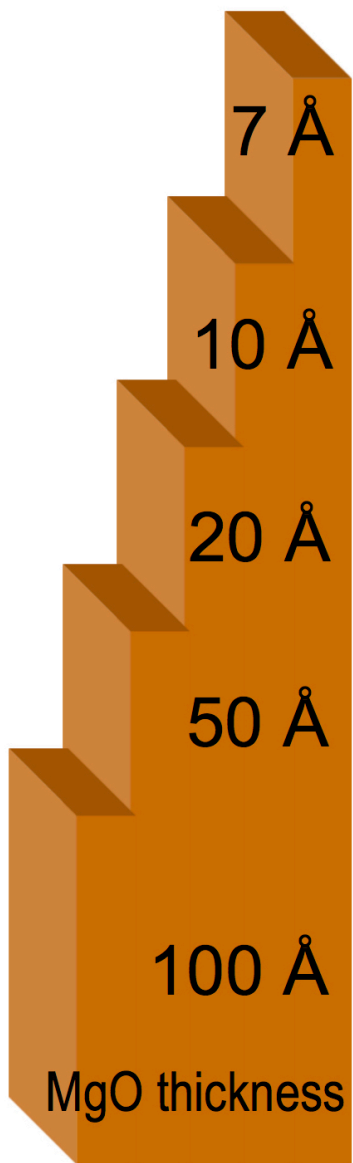


Fig. 1

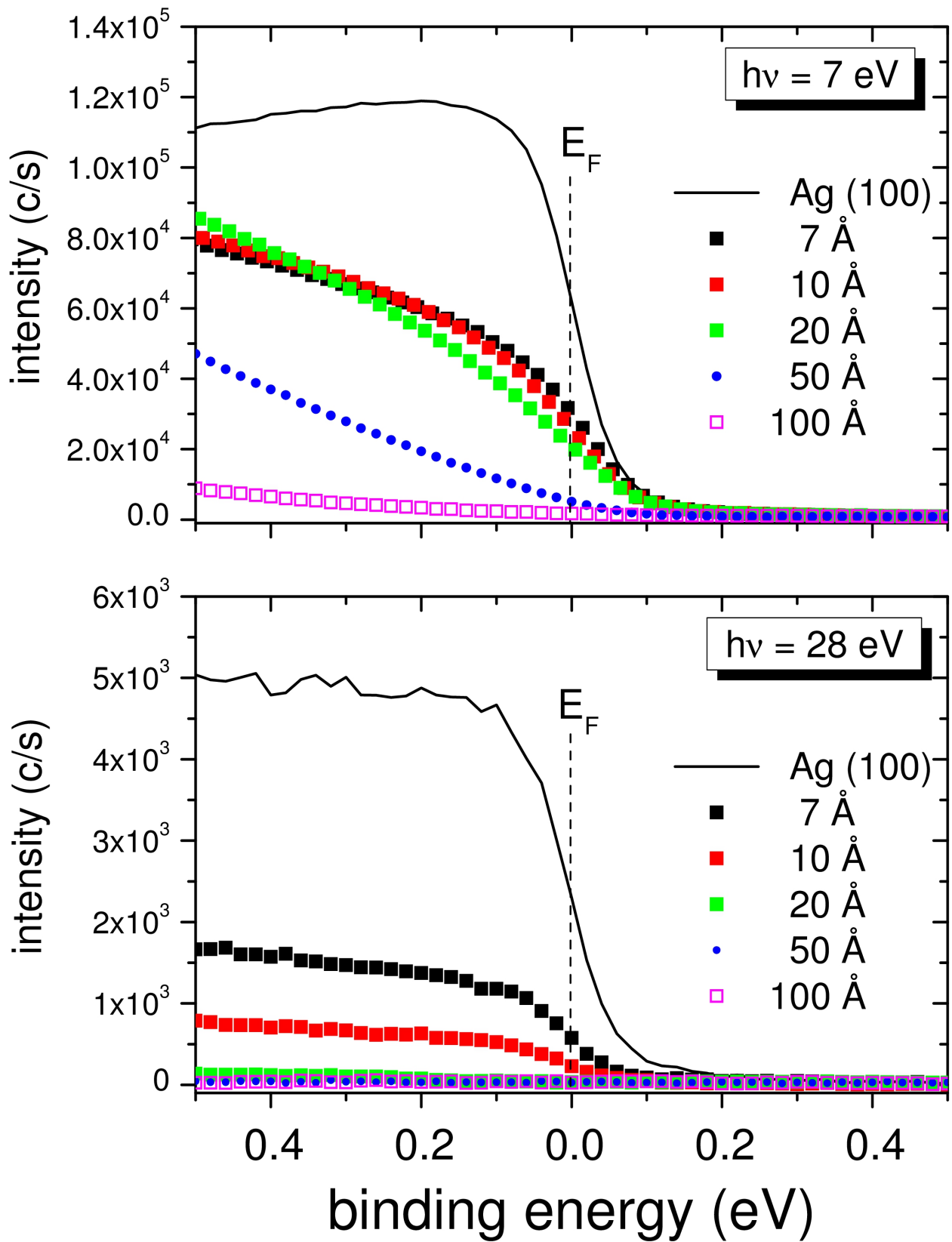


Fig. 2

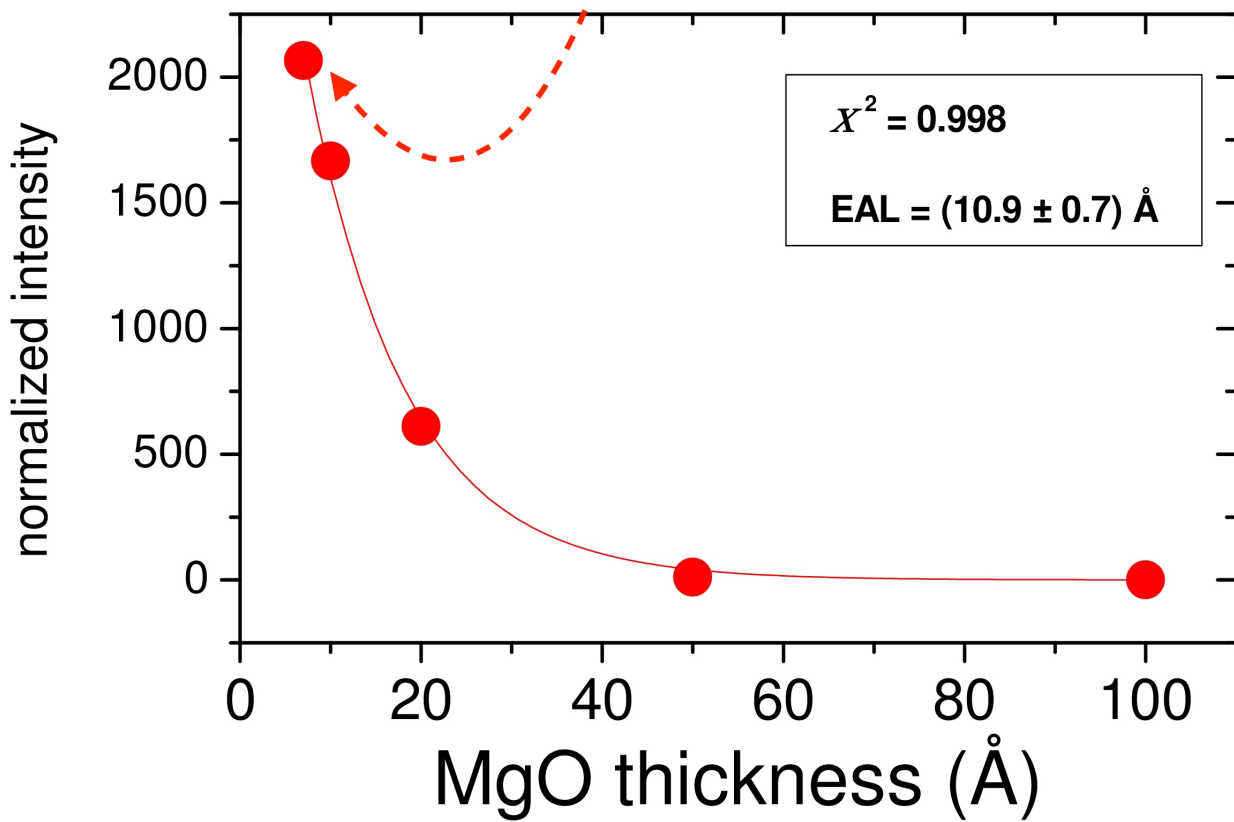
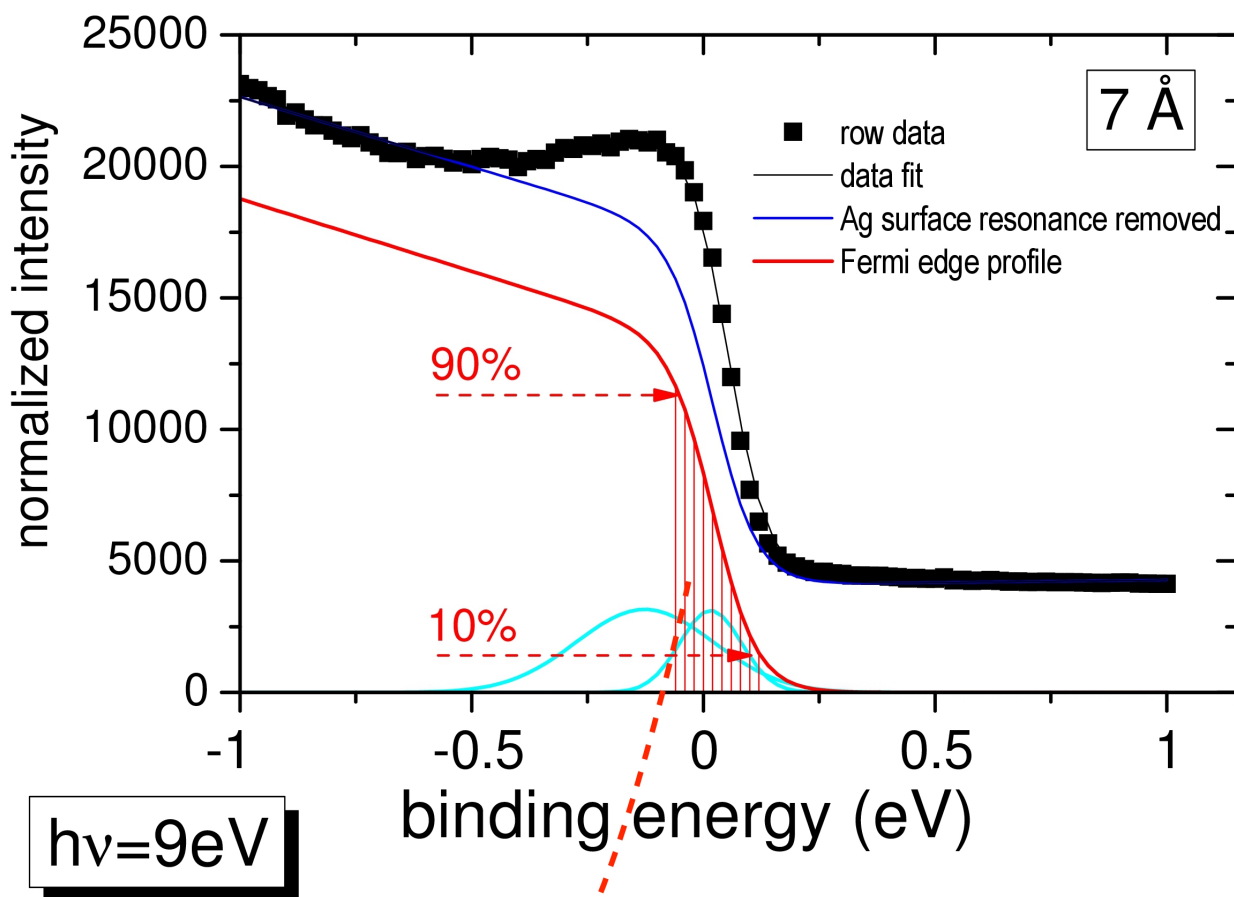


Fig. 3

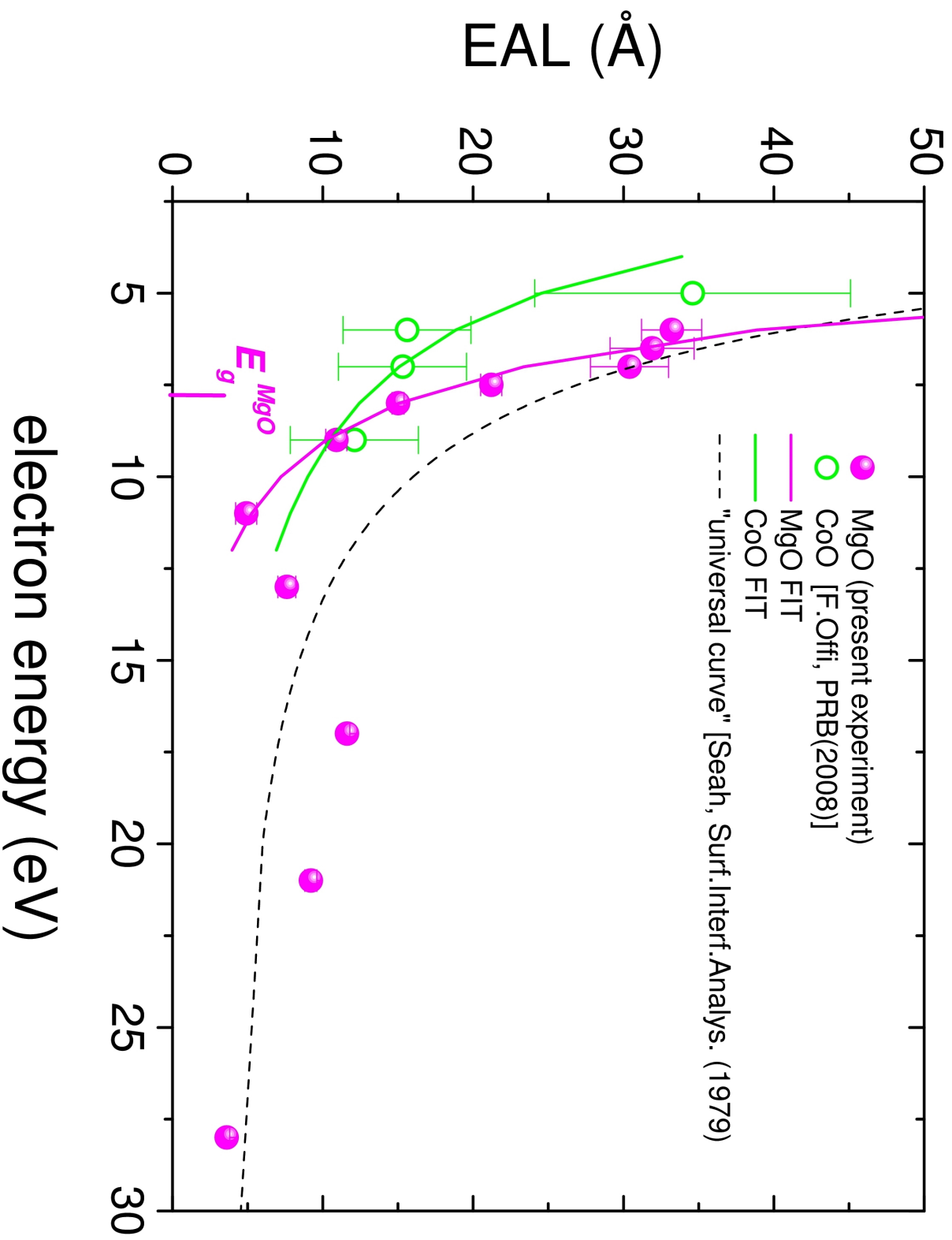


Fig. 4

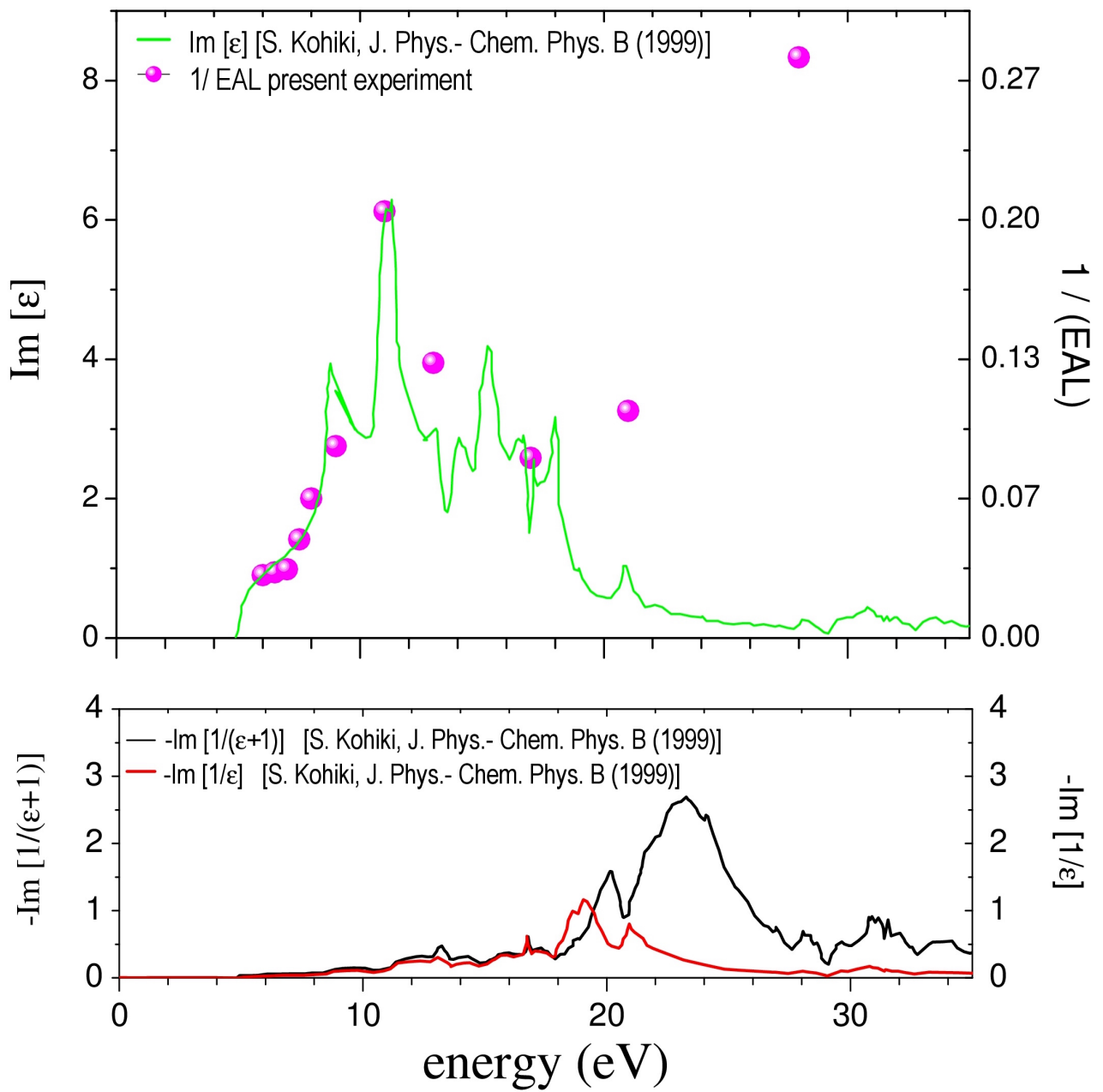


Fig. 5